Available online at www.sciencedirect.com
SCIENCE DIRECT®
Journal of the European Ceramic Society 24 (2004) 3713–3721
www.elsevier.com/locate/jeurceramsoc

Tin oxide nanoparticle formation using a surface modifying agent

L.R.B. Santos [a,b], T. Chartier [a], C. Pagnoux [a], J.F. Baumard [a], C.V. Santillii [b], S.H. Pulcinelli [b,*], A. Larbot [c]

[a] *Laboratoire de Science des Procédés Céramiques et Traitements de Surface (SPCTS)—UMR 6638 ENSCI, 47 à 73 Av. Albert Thomas, 87065 Limoges, France*
[b] *Instituto de Química, UNESP, P.O. Box 355, 14801-970 Araraquara, Brazil*
[c] *Laboratoire des Matériaux et Procédés Membranaire (CNRS-5635, UMII-ENSCM), 8 rue de l'École Normale, 34296 Montpellier Cedex 5, France*

Received 16 November 2003; received in revised form 19 February 2004; accepted 6 March 2004

Available online 8 May 2004

Abstract

This work presents results concerning the preparation of redispersible tin oxide nanoparticles achieved by using Tiron molecule ($(OH)_2C_6H_2(SO_3Na)_2$) as surface modifying agent. The adsorption isotherm measurements show that an amount of 10 wt.% of Tiron is need to recover the SnO_2 nanoparticles surface with a monolayer. These nanoparticles can be easily redispersed in tetramethylammonium hydroxide at pH $\geq$11 until a powder concentration of 12 vol.% of tin. Under these conditions, hydrodynamic particle size is about 7 nm and increases until 52 nm at pH 6 due to the aggregation phenomenon. The time evolution of the viscoelastic properties indicates that the suspensions at pH 12.5, containing 12 vol.% tin oxide and 10 wt.% of surface modifier are kinetically stable. After thermal treatment at different temperature the powder characterisation evidences that the presence of Tiron monolayer at the nanoparticles surface increases the thermal stability of the porous texture and prevent the micropore size growth. This set of results contributes to satisfy the demand for more controlled synthesis of nanoparticles with high thermal stability as required for fabrication of ultrafiltration ceramic membranes.

Keywords: Membranes; Sol–gel processes; SnO_2; Powders; Chemical preparation

1. Introduction

Recently, we have shown that SnO_2 membranes prepared by sol–gel route have microstructural and permeation properties adequate for applications in ultra and nanofiltration processes.[1] Nanofiltration results have indicated that this membrane can be employed for water desalinisation process.[2] Furthermore, thin SnO_2 layers present a dynamic scaling pore growth during sintering due to grain coalescence.[3] Permeation tests did in SnO_2 membranes have evidenced that this self-similar pore growth did not cause changes in the total porosity, tortuousity, and pores shape. According, SnO_2 membranes could satisfy the demand for controlled pore size distribution in all pore size ranges used for ultra and nanofiltration applications.[2]

The main problem in the preparation of supported ceramic membranes by the sol–gel process lies in the preparation of thick coatings (>1 μm), which may crack during postsynthesis drying and sintering steps.[4] The main cause of cracks formation and propagation is the low particle concentration in the initial suspension, due to a low powder redispersibility, that leads to a large shrinkage of the gel layer deposited on the stiffen support. In this case, the tendency to crack formation increases with the gel layer thickness and with the surface tension. Thus, to fabricate advanced nanostructured membranes for nano and ultrafiltration an adapted surface chemistry of particles is required to achieve a high redispersibility. For that a colloidal suspension with high nanoparticle concentration and low surface tension has to be used. These conditions can be achieved by adjusting the particle surface free energy by in situ surface modification during precipitation processes.[5] In aqueous media, organic compounds are widely used to improve the stability of colloidal suspensions because both steric hindrance and electrostatic repulsion can contribute to the dispersion.[6] These

* Corresponding author.
E-mail address: sandrap@iq.unesp.br (S.H. Pulcinelli).

0955-2219/$ – see front matter © 2004 Elsevier Ltd. All rights reserved.
doi:10.1016/j.jeurceramsoc.2004.03.003

organic surfactants have a long molecular chain, as large as the nanoparticles used in the preparation of the nanoscaled materials, and the volume occupied by these classical surfactants limits the powder concentration in suspension. Recently, Pagnoux et al.[7] have shown that the stability of aqueous alumina suspension can be greatly improved using small molecules, like Tiron (11 $Å^2$), as dispersant. Tiron molecules form chelate rings with ions of the alumina particle surface leading to a strong adsorption and, on second hand, the ionised groups develop a surface charge, which induces a high repulsive potential.[8,9]

This paper describes the preparation of redispersible nanoscaled tin oxide powders using Tiron molecules as surface modifying agent, the suspension properties and the improvement of the thermal stability of the derived powder covered by a monolayer of this surfactant.

2. Experimental

2.1. Powder preparation

The tin oxide nanoparticles were prepared by sol–gel route[10] using the controlled growth technique.[5,11] A concentrated aqueous ammonia solution was added to tin(IV) chloride ($SnCl_4 \cdot 5H_2O$, Aldrich) aqueous solution at 0.63 mol L^{-1} containing different concentration (1–20 wt.%, with respect to the tin oxide) of the surface modifying agent Tiron (4,5-dihydroxy-1,3-benzene disulfonic acid, disodium salt, Aldrich, France). The precipitate was kept under reflux at 100 °C for 90 min, and the chemically modified surface powder isolated by centrifugation at 14,000 × g for 15 min, and washed with bidistilled water. The concentration of the free Tiron was measured by UV absorption (wavelength: 290 nm) of supernatant liquid after centrifugation. The centrifugation–washing procedure was repeated several times to eliminate the remaining ions of the reaction. The concentration of the remaining ions, mainly chloride, at the end of the washing step was lesser than the detection limit of the specific chloride electrode ($\approx 10^{-5}$ mol L^{-1}). After drying at 80 °C for 12 h the powdered samples were characterised.

2.2. Characterisation

Electrophoretic measurements provide information on the nanoparticles surface charge. The electrophoretic mobility of redispersed tin oxide particles in presence of different amounts of Tiron was measured as a function of pH using a Coulter Delsa 440 equipment. A colloidal suspension containing 3 vol.% of solid was prepared by redispersing the dried powder in 0.5 mol L^{-1} alkaline aqueous solution. Tetramethylammonium hydroxide, TMAH, or ammonium hydroxide was used to adjust the initial alkaline pH. Subsequently, the pH of the dispersion was adjusted with hydrochloric acid. The zeta potential (ζ) was calculated using the Smoluchowski equation.[12] During the measurements, the current intensity, the frequency and the working temperature were fixed at 0.1 mA, 250 Hz and 25 °C, respectively. These dispersions were used to measure the hydrodynamic size of the particles, carried out by quasi-elastic light scattering, QELS (MALVERN 4700, $\lambda = 633$ nm).

The evaluation of the viscoelastic properties of the suspension containing nanoparticles was performed using a controlled stress rheometer (Carri-Med-CLS 100), with cone-plate configuration. The angular frequency, the torque, the displacement, and the temperature were kept constant at 2.6 rad s^{-1}, 100 μN m, 1 mrad and 15 °C, respectively.

The IR spectra of the powders containing different Tiron concentrations were measured in a wavenumber range from 400 to 4000 cm^{-1} with a Fourier transform infrared (FTIR) spectrometer (Perkin-Elmer 1760X) using KBr pellets containing 0.5 wt.% of powdered sample. The thermal behaviour of powder was investigated by DTA/TG (Rigaku PTC-10A) at heating rate of 10 °C min^{-1} under flowing air condition.

The BET surface area and the porous structure of samples containing different Tiron concentration were evaluated by N_2 adsorption isotherms measurements at 77 K and relative pressure interval between 0.001 and 0.998 (ASAP 2010, Micrometrics). Before each measurement, the samples were degassed at 80 °C under vacuum (10^{-3} mmHg) for time enough (12 h $< t <$ 18 h) to observe the absence of significant change in vacuum stability. Mesopore size distribution was evaluated from the desorption branch of the isotherms by using the capillary condensation model assuming cylindrical pores (BJH method)[13] and the microporosity was evaluated using a micropore algorithm.[14]

3. Results and discussion

3.1. Suspension properties

Fig. 1 presents the hydrodynamic size of particles and zeta potential as a function of pH corresponding to the powder containing 10 wt.% of Tiron redispersed in TMAH solution. An increase of the hydrodynamic size from 7.5 to 55 nm is verified as the pH decreases from 11 to 6. At the same time the zeta potential changes from ≈−30 to ≈−13 mV, leading to a decrease of the electrostatic repulsion between tin oxide particles, and agglomeration takes place. Thus the variation of the hydrodynamic size as a function of pH can be attributed to the state of agglomeration of particles.

The powders prepared with an amount of Tiron larger than 10 wt.% can be easily redispersible at pH ≈9.5 using a NH_4OH aqueous solution until 5.4 vol.% of powder. In this solution the hydrodynamic size of colloidal particles increases from 8 to 100 nm as the pH decreases from 9.5 to 7.6. For powders prepared with a Tiron concentration lower than 10 wt.%, higher values of pH are necessary to achieve a satisfactory redispersion. A 0.5 mol L^{-1} TMAH solution

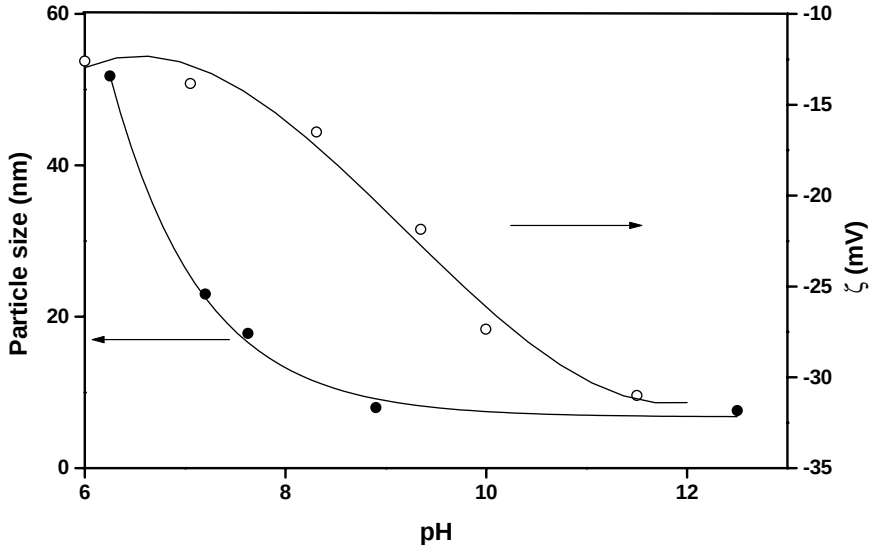

Fig. 1. Hydrodynamic size of particles (●) and zeta potential (○) as a function of the pH for the suspension prepared with SnO_2 powder containing 10 wt.% of Tiron.

at pH ≈12.5 was used to obtain the maximal SnO_2 powder redispersion. Then, it is possible to obtain a kinetically stable colloidal suspension for all the tested Tiron concentrations (5 wt.% < [Tiron] < 20 wt.%) with a solid content ranging from 5.4 to 12 vol.% by using NH_4OH (at pH 9.5) or TMAH (at pH 12.5), respectively.

The hydrodynamic size obtained for the samples prepared with Tiron amount larger than 10 wt.% stays approximately invariant (8 nm at pH 12.5), suggesting that the surface of tin oxide particles is completely covered by Tiron molecules and that an additional amount of Tiron does not change the agglomeration state of the fresh suspension. In order to confirm the monolayer capacity of SnO_2 nanoparticles, a Tiron adsorption isotherm was determined and plotted in Fig. 2. The amount adsorbed was calculated from the difference between the quantity of Tiron added and the remaining in the supernatant liquid after the reflux step. The curve presents a plateau for equilibrium concentration of Tiron higher than 0.024 mol L^{-1}, which corresponds to 10 wt.% of Tiron in a suspension containing 14.3 wt.% of powder. The shape of the curve is typical of Langmuir isotherms, in which the plateau corresponds to the monolayer capacity. Applying the Langmuir model[13] to experimental data, a monolayer capacity of 1.4×10^{-6} mol m^{-2} was calculated. This

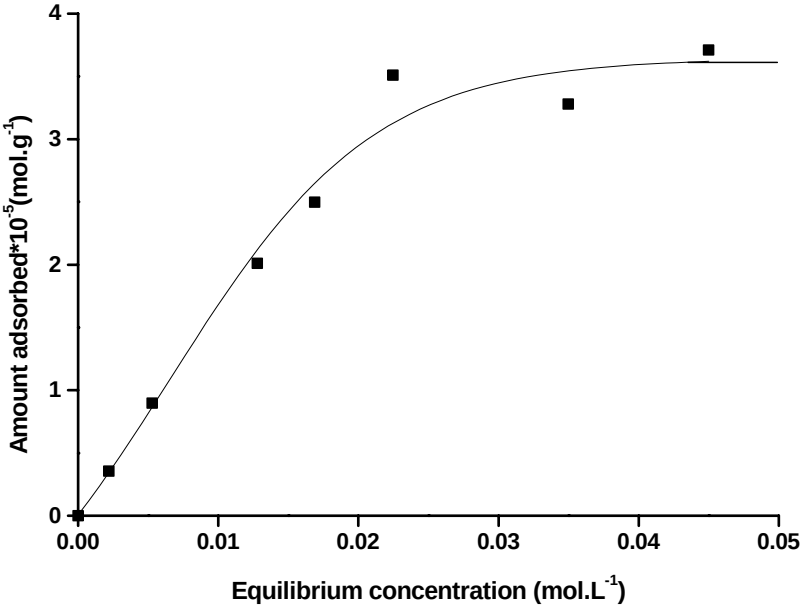

Fig. 2. Adsorption isotherm of Tiron molecules on tin oxide nanoparticles.

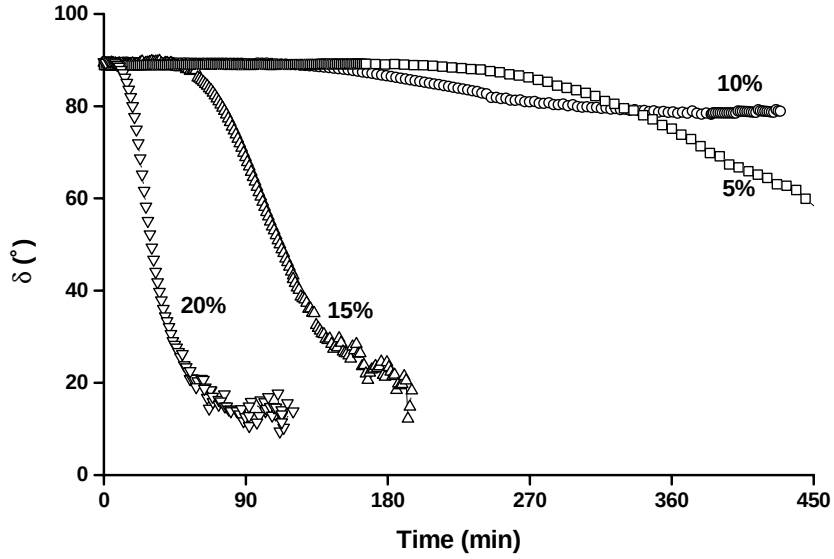

Fig. 3. Time evolution of the phase angle ($\tan\delta(\omega) = G''(\omega)/G'(\omega)$) for SnO_2 suspensions (12 vol.%) containing different Tiron concentrations at pH 12.5.

monolayer capacity is in good agreement with the value of 1.5×10^{-6} mol m^{-2} calculated by taking account for the cross section of a Tiron molecule (11 Å^2),[8] and the measured BET surface area (125 m^2 g^{-1}) of SnO_2 powder.

Information on the kinetic stability of the colloidal suspension was obtained by measuring the viscoelastic properties. Fig. 3 shows the time evolution of the phase angle (δ) for the suspensions containing 12 vol.% of nanoparticles redispersed in TMAH aqueous solution at pH 12.5 using powders with different Tiron concentrations. The phase angle is defined by

$$\tan\delta(\omega) = \frac{G''(\omega)}{G'(\omega)} \quad (1)$$

where G'' and G' are loss and storage moduli at a determined angular frequency (ω), respectively.

For samples containing 5 wt.% of Tiron, the phase angle decreased from 90° (typical of Newtonian fluid) to 79° after 45 min, indicating an increase of the agglomeration state. The minor temporal evolution of phase angle was observed for the suspension prepared with 10 wt.% of Tiron. This sample keeps the Newtonian behaviour for a long time period, evidencing the highest colloidal stability of the monolayer covered particles. The samples prepared with 15 or 20 wt.% of Tiron exhibit faster decrease of the phase angle, from 90 to 14° in about 90 min. This transformation, from a viscous fluid to an elastic solid-like behaviour, is related to the material structuration due to a network formation, typical of the sol–gel transition. Specifically, the sol–gel transition of SnO_2 colloidal suspension prepared by sol–gel route is the result of an aggregation process.[15] The primary particles become interconnected by hydrogen bonding between water molecules and superficial OH^- groups, giving rise to the formation of a continuous network of interlinked aggregates with a fractal structure.[15] Thus, the results obtained for samples prepared with [Tiron] > 10 wt.% indicate that the presence of free Tiron hinders the kinematical stability of the suspension, favouring the fast gelation. This effect can results from the decrease of the electrostatic repulsion between particles due to the increasing amount of sodium ion bonded to the ionic group (SO_3^-) of adsorbed Tiron molecules.

3.2. Powder properties

In order to understand the role of the Tiron molecules on the tin oxide surface, IR analysis of powders, dried at 110 °C, containing different Tiron concentrations were performed (Fig. 4a). The presence of bands concerning the surfactant is verified for all samples. The relative intensity of peaks concerning Tiron molecule increases up to a concentration of 10 wt.% and remains almost constant for higher amounts.

The bands corresponding to Tiron FTIR spectrum are assigned as follows[16,17]: the rings carbon–carbon stretching, $\nu_{C=C}$, vibrations are apparent at 1596, 1459 and 1426 cm^{-1}, out-of-plane ring deformation, $\delta_{(C=C)op}$ in between 490 and 520 cm^{-1}, the carbon–hydrogen stretching, ν_{CH}, at 3091 cm^{-1}, and out-of-plane deformation, $\delta_{(CH)op}$, at 847 cm^{-1}; a broad band in the region of 3600–3100 cm^{-1} shows the ν_{OH} vibrations splitted into three peaks, at 3546, 3495 and 3274 cm^{-1}, probably due to the presence of intermolecular hydrogen bonding, while the δ_{OH} are apparent at 1639 cm^{-1}, the in-plane deformation, $\delta_{(OH)ip}$ and the ν_{CO} are coupled together resulting in a couple of bands located at 1283 and at 1224 cm^{-1}. The band with shoulder at 1034 cm^{-1} and the broad band at 1185 cm^{-1} are assigned to symmetric and asymmetric stretching vibration of SO_3Na, respectively, while the peak at 1094 cm^{-1} is usually attributed to ionic sulphates impurities.[9,16,18] The stretching vibrations of SO_3^- groups is difficult to assign due

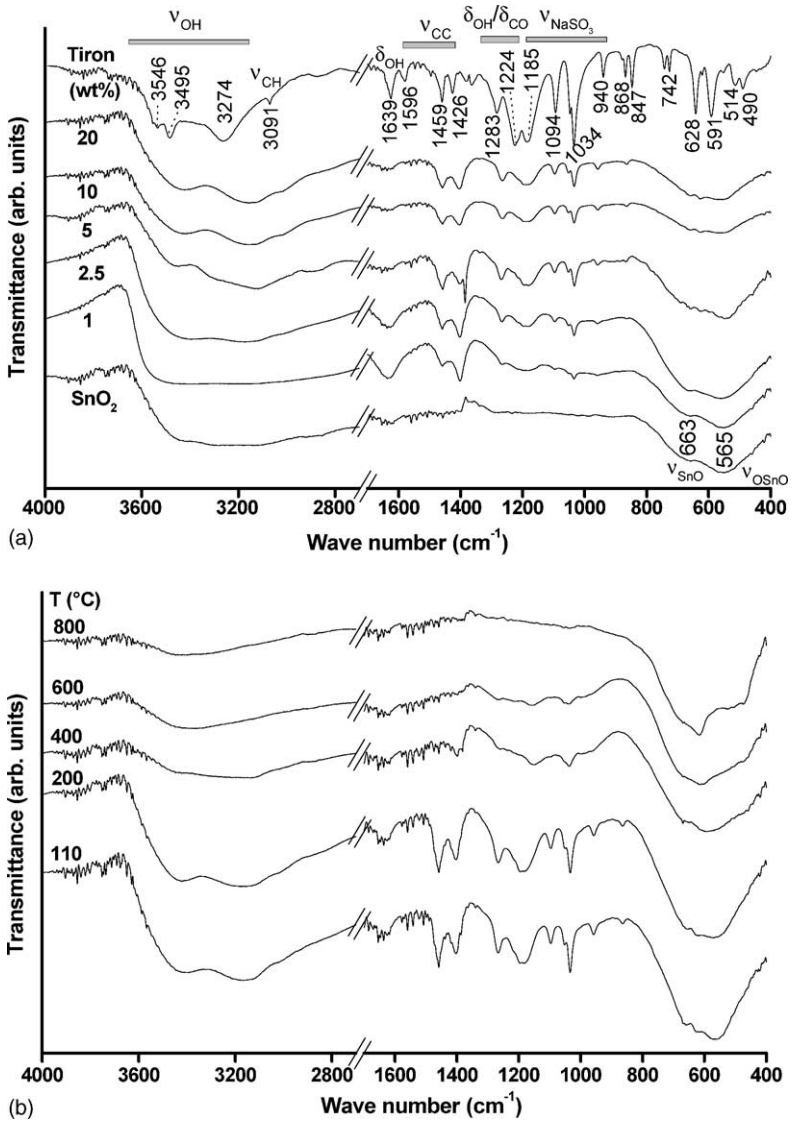

Fig. 4. FTIR spectra of (a) tin oxide powders prepared with different Tiron concentrations and (b) tin oxide samples containing 10 wt.% Tiron treated at different temperatures for 1 h.

to the occurrence of CH vibrations in the same frequency regions,[9,16] i.e. the SO stretching appears at 940 cm^{-1} and the bending at 630 and 495 cm^{-1}. The splitting of the last band in two components may characterise the ionic bonding of sodium.[16]

Tin oxide FTIR spectrum shows the presence of stretching vibrations bands ν_{OSnO} and ν_{SnO} at 663 and 565 cm^{-1}, respectively.[19,20] A broad band centred at almost 3500 cm^{-1} coupled to that at almost 1640 cm^{-1}, characteristic of water stretching and bending are also apparent. The broadening and the shape of the bands in the region from 400 to 800 cm^{-1} is often observed for nanocrystalline cassiterite xerogels, having surface hydroxyl groups.[19–21] According to Giuntini et al.[21] the relative intensity change of $I\nu_{SnO}/I\nu_{OSnO}$ bands could be correlated to the rearrangement occurring during firing of SnO_2 xerogels.

The comparison of FTIR spectra of Tiron, SnO_2, and SnO_2 containing increasing concentration of Tiron revealed:

(i) The position and relative intensity of peaks observed in between 1000 and 1200 cm^{-1}, corresponding to stretching frequencies of the SO_3Na groups remains almost unchanged, suggesting that the sulphate group was not involved in a dominant way with the immobilisation of Tiron molecules.
(ii) The ν_{OH} at almost 3500 cm^{-1} is not observed in spectra of Tiron–SnO_2 xerogels, and the two bands between 1200 and 1300 cm^{-1}, corresponding to the coupled vibration $\nu_{CO}/\delta_{(OH)ip}$, collapses into a single one at 1264 cm^{-1}. It indicates the immobilisation process occurs by coordination of the two oxygen atoms of Tiron molecule.

(iii) The increase in intensity and the shift to higher vibration energy of $\nu_{C=C}$ peaks at 1459 and 1426 cm^{-1} suggest that this immobilisation involves the formation of chelate rings.
(iv) The decrease of the relative intensity of peaks, $I\nu_{SnO}/I\nu_{OSnO}$, is indicative of the planar arrangements of the O–Sn–O bridges formed by the elimination of hydroxyl surface groups.[20,21]

This behaviour gives strong evidence that the immobilisation process occurs by the chelation of Tiron molecules at the surface of SnO_2 nanoparticles. Under basic pH as used in our syntheses, the surface of nanoparticles is negatively charged hindering the immobilisation of Tiron by SO_3^- groups. According, the immobilisation of Tiron molecules occurs in predominant way by the formation of surface chelate, due to the reaction between alcohol groups of the molecule and hydroxyl groups at the surface of particles. On the other side, due to the presence of Tiron SO_3^- groups at surface of tin oxide nanoparticles, an increase of the charge density is verified and the redispersibility property of the tin oxide powders favoured.

Fig. 4b presents the FTIR spectra of powders containing 10 wt.% of Tiron dried at 110 °C and treated at different temperatures for 1 h. For the samples treated between 110 and 400 °C, the bands attributed to surfactant are observed. Above 400 °C the bands characteristic of Tiron gradually disappear, as the firing temperature increases. The bands at 1495 and 1401 cm^{-1}, attributed to the C=C stretching frequency are the first that disappear, followed by those between 1295 and 1100 cm^{-1}, concerning SO_3^- stretching of SO_3Na group. This thermostability of Tiron immobilised at the surface of SnO_2 nanopaticles is a complementary evidence of the chelate complex formation involving the hydroxyl groups in the *ortho*-position of aromatic ring and tin atoms at the surface of nanoparticles. Another interesting point revealed by these spectra is the slow decrease of the intensify ratio $I\nu_{SnO}/I\nu_{OSnO}$ as a function of the firing temperature. Several studies done on ungrafted SnO_2 xerogels[19–21] have shown that this ratio decreases to values smaller than the unity by firing at temperatures higher than 350 °C. Our results show that the intensity of ν_{SnO} band becomes lower than that of ν_{OSnO} only for sample fired above 600 °C, suggesting that the crystallite growth is inhibited by the Tiron surface modification. This feature is in agreement with the idea early proposed by Wu et al.[22] concerning the thermostabilisation of sol–gel derived nanocrystalline metal oxides by using OH-scavenging reagent enable to replace the hydroxyl groups and form non-condensing functionalised surface.

This thermodecomposition behaviour was confirmed by TGA and DTA analysis of dried SnO_2 powder prepared with 10 wt.% of Tiron (Fig. 5), that shows the decomposition of Tiron occurs near to 400 °C. The TGA curve exhibits two apparent weight losses. The first one between room temperature and 150 °C is likely due to the loss of the residual solvent and water remaining in the as-dried powder, as evidenced by the endothermic peak in the DTA curve at the same temperature range. The second weight loss, between 150 and 350 °C, may be due to the initial step of decomposition of grafted Tiron molecules. A strong exothermic peak at 375 °C in the DTA curve confirms the combustion of the surfactant derivatives. For temperatures higher than 400 °C low weight loss is observed, indicating the completion of removal of Tiron derivatives.

The evolution of the powder texture after different heat treatments is evidenced by changes of the N_2 adsorption–desorption isotherms shown in Fig. 6a. The high volume of gas adsorbed at low relative pressure (p/p_0), the plateau at high p/p_0-range, and the absence of hysteresis in curve corresponding to sample treated at 400 °C is typical

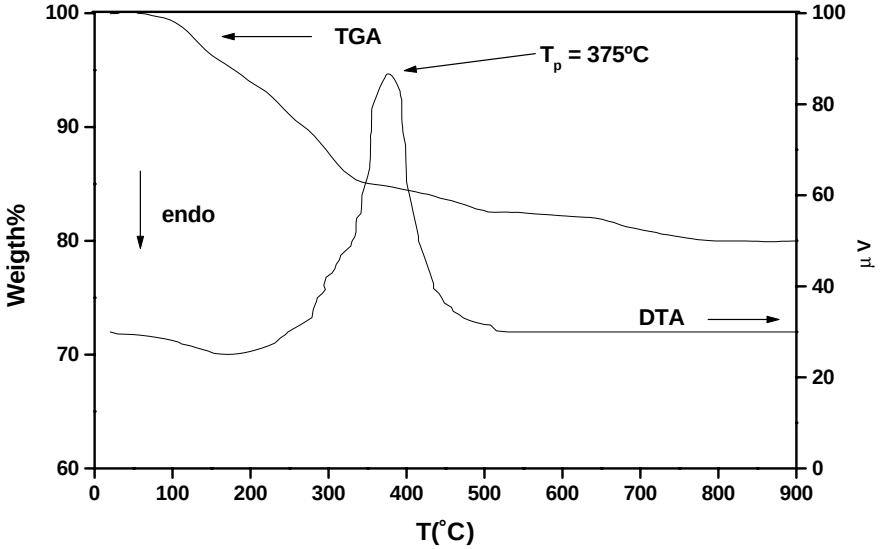

Fig. 5. DTA and TG analysis of the dried tin oxide powder prepared with 10 wt.% of Tiron.

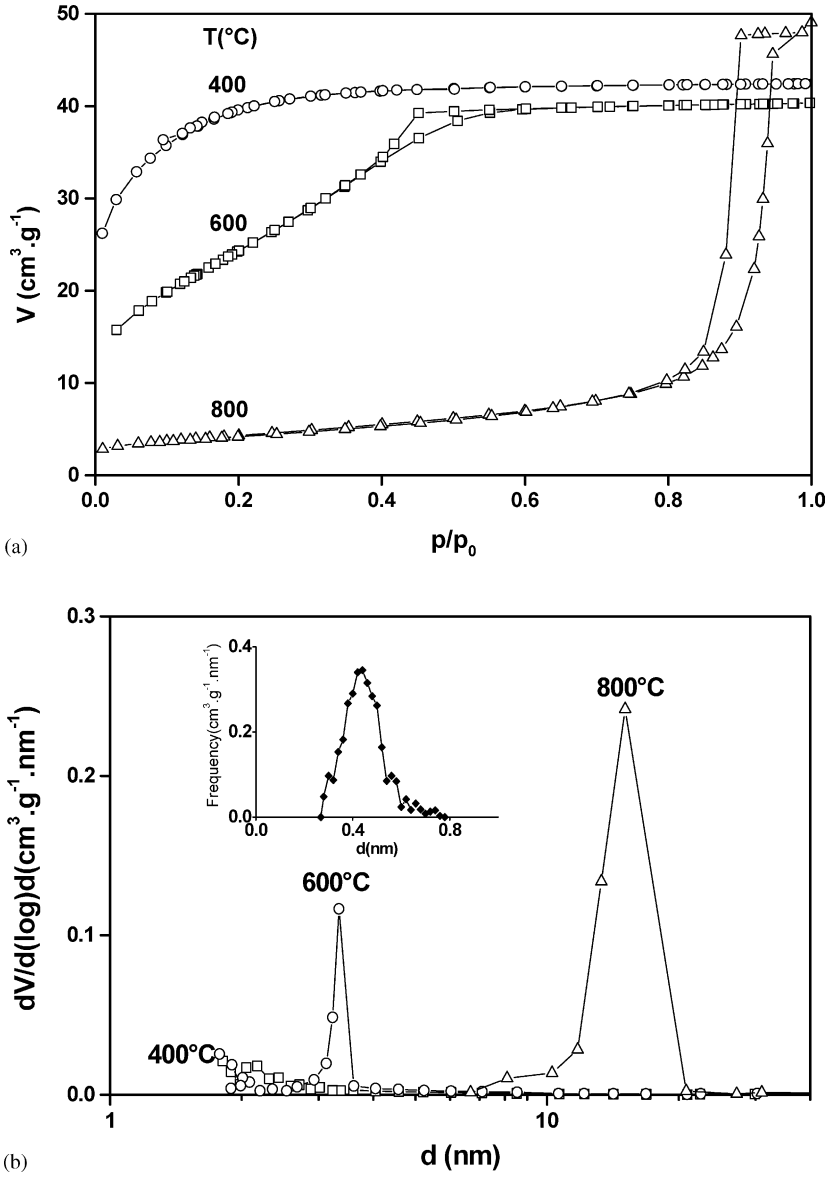

Fig. 6. (a) N_2 adsorption–desorption isotherms and (b) evolution of the pore size distribution for powders prepared with 10 wt.% of Tiron treated during 1 h at different temperatures. The inset presents the microporous size distribution of the sample treated at 400 °C.

of materials presenting micropores (type I isotherm, according to IUPAC classification[13]). Above this temperature isotherms become characteristic of type IV, with hysteresis loop type H2 and H1 for samples treated at 600 and 800 °C, respectively. This hysteresis loop evolution indicates that the regularity of cross section along the longitudinal direction of pores increases by increasing the firing temperature. In an idealised description this is equivalent to the transformation from inkbottle towards cylindrical shaped pores.[1] This overall behaviour of porous texture has already been observed with undoped[1] and doped[23] SnO_2 xerogel prepared in absence of surfactant. However, there are some interesting differences. In absence of surfactant the H2 hysteresis loop, typical of capillar condensation inside mesopores, appears in samples fired at relatively low temperature (300 °C), while for Tiron modified xerogel it occurs after firing at 600 °C. This increase in thermal stability of micropores is a clear evidence that Tiron reduces the surface free energy of SnO_2 nanoparticles.

The pore size distribution curves, calculated from desorption branches (Fig. 6b), make evident that by increasing the treatment temperature the average pore diameter shifts from 3.5 (600 °C) to 10.5 nm (800 °C), while the pore volume remains constant. The inset, representing the sample treated at 400 °C for 1 h, shows the pore size distribution with average pore size of 0.4 nm, determined by MP method.[13] Analogous micropore size distribution was verified for samples fired at lower temperatures. More than pore growth, the BET surface area decreases from 138 to 15 $m^2\,g^{-1}$, while the pore value stays invariant

($\cong 0.065\,m^2\,g^{-1}$) as the firing temperature increases from 400 to 800 °C. This overall behaviour is in agreement with the dynamic scaling growth mechanism proposed by Santilli et al.[3] However, in absence of surfactant the change in surface area and pore size is about three times more important for the SnO_2 xerogel fired in the comparable temperature range.[1,23]

These results confirm that the presence of Tiron molecules, added before the precipitation step during the powder preparation process, leads to control the particle and pore size growth. This feature is consistent with the mechanism of particles coalescence controlled by the surface mobility proposed for SnO_2 xerogel.[23,24] In this case the presence of Tiron adsorbed layer, as well as of inorganic compound,[23] decreases the surface energy and consequently reduces the surface mobility of nanoparticles. In fact, this feature can be explained by two mean effects of Tiron as surface modifier: (i) the condensation reaction involving surface hydroxyl groups do not occur due their replacement by chelated molecule, and (ii) the nanopartitcles are isolated by the Tiron adsorbed layer restricting the grain boundaries motions. These aspects of the surface modifying tin oxide nanoparticles are particularly important in membrane technology because they allows to prepare nanofiltration tin oxide membranes with high thermal stability.

4. Conclusions

Nanoscaled tin oxide particles, which are fully redispersible in water in alkaline medium, were prepared. The growth of particles in solution was controlled by chemical surface modification of the tin oxide nanoparticles using Tiron as surface modifier.

The concentration for which the tin oxide surface is covered by a monolayer of chemical surface modifier is about $3.5 \times 10^{-5}\,mol\,g^{-1}$. Above this value small modifications occur in the powder redispersibility and the kinetics stability of dispersion decreases.

A pH $\geq$12 is required to obtain a stable suspension of SnO_2 powder prepared with Tiron concentration lower than 10 wt.%. On the other hand, an ammonium aqueous solution at pH $\approx$9.5 is sufficient to disperse SnO_2 nanoparticles prepared with 10 wt.% of the Tiron. The hydrodynamic size changes from 7 to 51 nm when pH changes from 12 to 6 due to the increase of aggregation state.

The presence of Tiron molecules on the surface of the tin oxide particles minimises the effect of grain coalescence during the heat treatment so that microporous materials can be obtained. This aspect of the surface modification synthesis is especially important to obtain new SnO_2 nanofiltration membranes. By increasing the treatment temperature from 400 to 800 °C, the pore size of xerogels can be continuously screened from 0.4 to 10 nm in a controlled way.

Acknowledgements

This work has been supported by CAPES/COFECUB, FAPESP and PRONEX, Brazil.

References

1. Brito, G. E. S., Pulcinelli, S. H. and Santilli, C. V., Pore size distribution on unsupported SnO_2 membranes prepared by sol–gel process. *J. Sol–Gel Sci. Technol.* 1994, **2**, 575–579.
2. Santos, L. R. B., Larbot, A., Santilli, C. V. and Pulcinelli, S. H., Study of the selectivity of SnO_2 supported membranes prepared by a sol–gel route. *J. Sol–Gel Sci. Technol.* 1998, **13**, 805–811.
3. Santilli, C. V., Pulcinelli, S. H. and Craievich, A. F., Porosity evolution in SnO_2 xerogels during sintering under isothermal conditions. *Phys. Rev. B* 1995, **51**, 8806–8809.
4. Santos, L. R. B., Pulcinelli, S. H. and Santilli, C. V., Preparationof SnO_2 supported membranes with ultrafine pores. *J. Membr. Sci.* 1997, **127**, 77–86.
5. Goebbert, C., Aegerter, M. A., Burgard, D., Nass, R. and Schimidt, H., Ultrafiltration conducting membranes and coatings from redispersable, nanoscaled, crystalline SnO_2:Sb particles. *J. Mater. Chem.* 1999, **9**, 253–258.
6. Pagnoux, C., Chartier, T., Granja, M. F., Doreau, F. and Ferreira, J. M., Aqueous suspensions for tape-casting based on acrylic binders. *J. Eur. Ceram. Soc.* 1998, **18**, 241–247.
7. Pagnoux, C., Serantoni, M., Laucournet, R., Chartier, T. and Baumard, J. F., Influence of the temperature on the stability of aqueous alumina suspensions. *J. Eur. Ceram. Soc.* 1999, **19**, 1935–1948.
8. Kummert, R. and Stumm, W., The surface complexation or organic acids on hydrous γ-Al_2O_3. *J. Coll. Interface Sci.* 1980, **75**, 373–385.
9. Jiang, L., Gao, L. and Liu, Y., Adsorption of salicylic acid, 5-sulfosalicylic acid and Tiron at the alumina–water interface. *J. Coll. Surf. A* 2002, **211**, 165–172.
10. Hiratsuka, R. S., Pulcinelli, S. H. and Santilli, C. V., Formation of SnO_2 gels from dispersed sols in aqueous colloidal solution. *J. Non-Cryst. Solids* 1990, **121**, 76–83.
11. Prakash, S. S., Brinker, C. J., Hurd, A. J. and Rao, M. S., Silica aerogel films prepared at ambient pressure by using surface derivatization to induce reversible drying shrinkage. *Nature* 1995, **374**, 439–443.
12. Hunter, R. J. *Colloid Science: Zeta Potential in Colloid Science Principles and Applications.* Academic Press, London, 1981, p. 465.
13. Gregg, S. J. and Sing, K. S. W. *Adsorption, Surface Area and Porosity*. Academic Press, London, 1982, p. 184.
14. Medek, J., Possibility of micropore analysis of coal and coke from the carbon dioxide isotherm. *J. Fuel* 1977, **56**, 131–133.
15. Santos, L. R. B., Santilli, C. V. and Pulcinelli, S. H., Sol–gel transition in SnO_2 colloidal suspensions: viscoelastic properties. *J. Non-Cryst. Solids* 1999, **247**, 153–157.
16. Socrates, G. *Infrared Characteristic Group Frequencies*. John Wiley & Sons Inc., London, UK, 1994.
17. Simmons, N. J., Aileen Chin, K. O., Harnisch, J. A., Vaidua, B., Trahanovsky, W. S., Porter, M. D. *et al.*, Synthesis and characterization of a catechol-terminated alkanethiolate monolayer adsorbed on gold. *J. Electroanal. Chem.* 2000, **482**, 178–187.
18. Pandit, B. and Chudasama, U., A new inorgano-organic ion exchanger: Tiron anchored to zirconium molybdate. *J. Chem. Res.* 1996, **5**, 2752–2767.
19. Ribeiro, S. J. L., Santilli, C. V., Pulcinelli, S. H., Fortes, F. J. P. and Oliveira, L. F. C., Spectroscopic characterization of SnO_2 gels. *J. Sol–Gel Sci. Technol.* 1994, **2**, 263–267.
20. Orel, B., Lavrencic-Stangar, U., Crmjak-Orel, Z., Bukovec, P. and Kosec, M., Structural and FTIR spectroscopic studies of gel–xerogel–oxide transitions of SnO_2 and SnO_2: Sb powders and

dip-coated films prepared via inorganic sol–gel route. *J. Non-Cryst. Solids* 1994, **167**, 272–288.
21. Giuntini, J. C., Granier, W., Zanchetta, T. V. and Taha, A., Sol–gel preparation and transport properties of a tin oxide. *J. Mater. Sci. Lett.* 1990, **9**, 1383–1388.
22. Wu, N. L., Wang, S. Y. and Rusakova, I. A., Inhibition of crystallite growth in the sol–gel synthesis of nanocrystalline metal oxides. *Science* 1999, **285**, 1375–1377.
23. Santilli, C. V., Pulcinelli, S. H., Brito, G. E. S. and Briois, V., Sintering and crystallitte growth of nanocrystalline copper doped tin oxide. *J. Phys. Chem. B* 1999, **103**, 2660–2667.
24. Briois, V., Santilli, C. V., Pulcinelli, S. H. and Brito, G. E. S., EXAFS and XRD analyses of the structural evolutions involved during drying of SnO_2 hydrogels. *J. Non-Cryst. Solids* 1995, **191**, 17–28.